T3P.132

DUAL-BEAM, SIX-TERMINAL NANOELECTROMECHANICAL RELAYS

K.L. Harrison[1], W.S. Lee[1], K. Shavezipur[2], J. Provine[1], S. Mitra[1], H.-S.P. Wong[1], R.T. Howe[1]
[1] Dept. of Electrical Eng., Stanford University, Stanford, California, USA
[2] Dept. of Food, Agricultural and Biological Eng., Ohio State University, Columbus, Ohio, USA

ABSTRACT

A novel design for a six-terminal nanoelectromechanical relay is presented. The design includes a secondary beam in the signal pathway of the device, which allows direct contact between the source and drain. The advantages of the new design include avoidance of fabrication-based contact degradation during the isolation etch, lower sensitivity to high gap variations and reduction in the number of contacts needed to close the signal pathway. Also, the new design introduces a novel anti-stiction mechanism. An analytical model is presented which compares the mechanical behavior of the new design to the older design. The devices are fabricated using a silicon nitride hard mask with an ammonium hydroxide based etchant. An inverter made using the new design is demonstrated.

KEYWORDS

relay, titanium nitride, nanoelectromechanical

INTRODUCTION

Nanoelectromechanical (NEM) relays have many advantages over CMOS transistors, including zero leakage current and high subthreshold slope [1]. Thus, NEM relays avoid many of the scaling problems encountered by CMOS devices. Furthermore, NEM relays may be fabricated on top of the CMOS layer by using a back-end-of-line-compatible process. By stacking relays on CMOS, the total footprint of a device can be reduced. An example of an integrated CMOS-NEM relay has been proposed which would replace some routing cells for an FPGA with NEM relays, yielding a significant reduction in footprint [4].

Laterally actuated relays with electrically isolated actuation and signal pathways were previously demonstrated [2]. Isolation allows the devices to be used as inverters and to be cascaded, and multiple devices can be used to implement digital circuits [3]. Disadvantages of previous lateral relay designs include contact degradation due to isolation overetch, high resistive loads due to two series electrical contacts, and sensitivity to gap variation. In this paper, we present a dual-beam NEM relay, which utilizes multiple flexible electrodes to reduce the number of ohmic contacts and move the isolation etch away from the signal pathway.

In the single-beam design presented in the previous work, a lateral relay consisted of a flexible beam called the gate, two body bias electrodes, a drain electrode and two source electrodes, as shown in Fig. 1. The gate deforms due to electrostatic force from the body bias electrodes and connects the source and drain. Current from the signal pathway cannot flow through the gate due to etching of the outer conductive layer, as shown in the figure. The gate must make contact with both the drain and source simultaneously to complete the signal pathway.

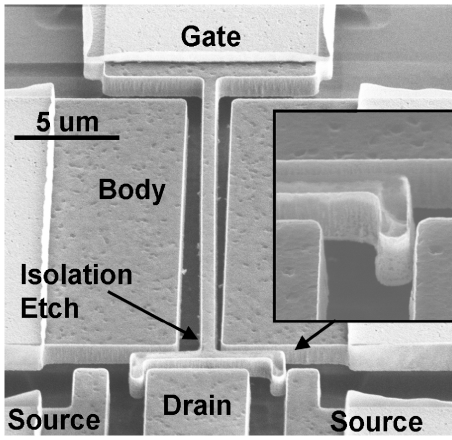

Figure 1: Single Beam design with rigid contact and isolation etch. Damage to the beam from the isolation etch can be seen in the inset picture.

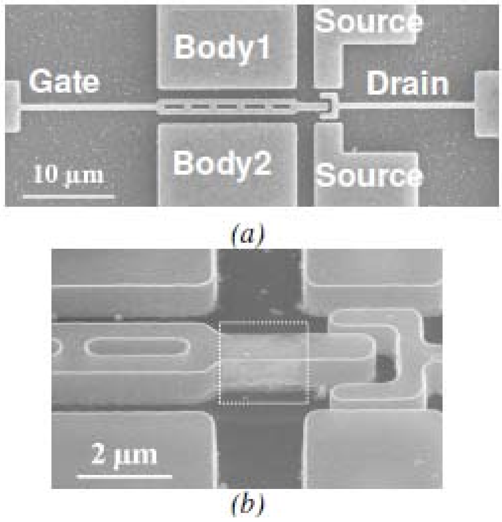

Figure 2: (a) SEM image of a dual-beam relay design; (b) SEM close-up image of the isolation etch area on the gate

We propose a new design for a symmetric, isolated six-terminal relay, which creates direct mechanical contact between the source and drain electrodes. In this design, shown in Fig. 2a, the gate exerts force on a flexible drain, which deforms and contacts the source directly. This dual-beam design has many advantages over the single-beam design:

- Reduces contact resistance by limiting the number of contacts in the signal pathway
- Mitigates the effect of gap size variation by decreasing the contact stiffness
- Reduces contact degradation by limiting isolation etch to the surface of a non-conducting beam

Furthermore, the new design introduces a novel post-stiction resurrection mechanism.

A disadvantage of the new dual-beam design could be higher actuation voltages due to the added force required to deform the drain and the larger distance between the gate and body. However, for greater unevenness in gap size, the dual-beam design will yield lower pull-in voltages. A second disadvantage is a larger device footprint due to the long, flexible drain beam.

ANALYSIS

For single-beam devices without an isolation etch, the pull-in voltages to the source (V_{PI_S}) and drain (V_{PI_D}) can be measured separately. An ideal device would pull-in to the two electrodes simultaneously. However, it has been shown that the gate makes contact with one electrode before the other [2]. This asymmetry in gap size may be due to physical wear, debris at the contact, roughness due to sidewall etching or film deposition, or deformation due to internal stresses. Figure 3 shows some examples of uneven sidewalls caused by (a) debris from sidewall etching and (b) mechanical wear of the contact surface after many operation cycles.

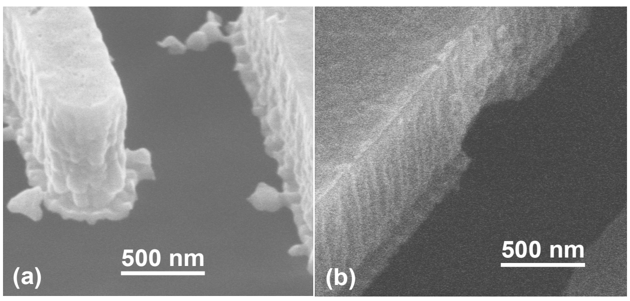

Figure 3: (a) SEM image of the sidewall of a device with debris from fabrication; (b) SEM image of sidewall deformed by wear

An alternative design features flexible source and drain electrodes, as shown in figure 4a. The flexible electrodes in the single-beam design would allow the first contact to deflect so that the gate could make contact with the second electrode. However, testing of these devices without isolation has proven that they still require high overdrive

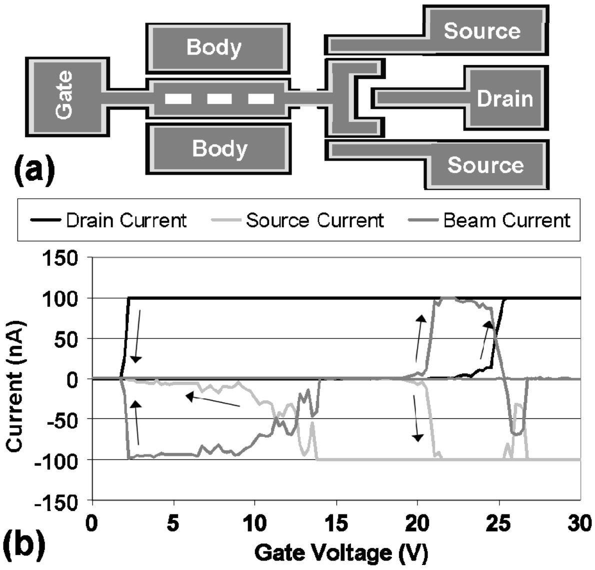

Figure 4: (a) Diagram of a single-beam device with elongated source and drain electrodes; (b) Results of electrical testing of single-beam device with elongated source and drain electrodes show staggered pull-in of beam and source at 20V and drain at 23 V.

voltage before the gate can make contact with both the source and drain electrodes, as shown in Figure 4b. The asymmetry would be exacerbated by internal stresses in the electrodes, which would cause bending of the flexible beams and therefore larger gap variations. This design also has two additional disadvantages: 1) Because of the flexibility of the electrodes, greater displacement is needed to break the contact during pull-out, making this design more vulnerable to stiction and welding. The low pull-out voltage in Figure 4b would suggest that adhesion forces are more pronounced; 2) The flexibility of the electrodes would allow the gate to make contact with the body electrodes, usually leading to permanent failure of the device. Therefore, the ideal design would have low enough contact stiffness to overcome gap variations but high enough stiffness to ensure pull-out and prevent shorting between body and gate electrodes.

A simple model can be used to compare the single-beam and dual-beam electrodes. Given contact gap sizes near 500 nm for 30 um long beams, the angle of rotation of the beam is very small. Therefore, the actuator can be described using parallel-plate electrostatic actuation models. A simple one DOF model is shown in Figure 5c. Assuming that the beams in the devices can be modeled as cantilever springs, the spring force F_K and actuation force F_E are given by:

$$F_K = \frac{3EI}{L^3} y \quad (1), \qquad F_E = \frac{1}{2} \frac{\varepsilon A}{(D_G - y)^2} V^2 \quad (2)$$

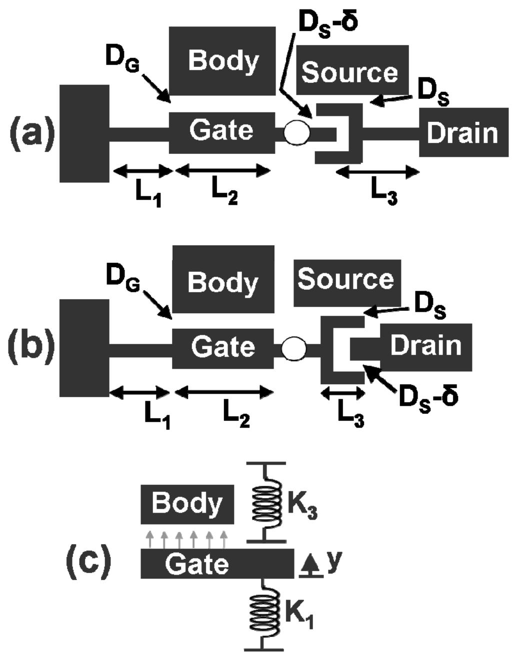

Figure 5: Diagrams of a (a) dual-beam device and a (b) single-beam device showing location of gap variation; (c) One DOF model of device actuations

where E is the Young's Modulus of the structural material (polysilicon), I is the moment of inertia, L is the length of the cantilever, y is the displacement of the rigid area of the gate, ε is the permittivity of the medium in the gap, A is the area of electrostatic actuation, D_G is the initial distance between the gate and the body electrodes and V is the actuation voltage. Both designs include a single rigid beam section that is electrostatically actuated and attached to two springs in parallel. Therefore, the force-balance equation for both designs is given by:

$$F_E = F_{K1} + F_{K2} \quad (3)$$

$$\frac{1}{2}\frac{\varepsilon A}{(D_G - y)^2}V^2 = \frac{3EI}{L_1^3}y + \frac{3EI}{L_3^3}(y - D_S) \quad (4)$$

where D_S is the designed contact gap size.

In the dual-beam design, the secondary spring K_3 models the flexible drain electrode and pull-in occurs at $y = 2{*}D_S + \delta$. In the single-beam design, K_3 models a single tine at the end of the gate electrode and pull-in occurs at $y = D_S + \delta$. Although the total actuation distance is larger for the dual-beam design, the secondary spring is more flexible. Therefore, there must be a value of gap variation δ' above which the dual-beam design has a lower pull-in voltage than the single-beam design. Figure 6 shows a graph of pull-in voltage vs. gap size variations for both designs using material and dimensional values from the fabricated devices. The analysis shows that δ' occurs below 10 nm, which is

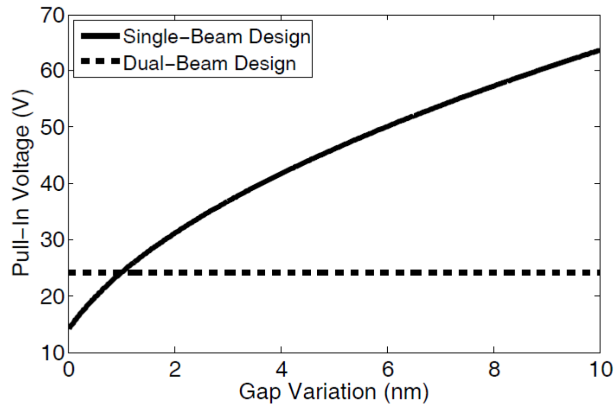

Figure 6: Graph of Pull-in voltage versus gap variation.

within the range of gap variation that has been observed in real devices. Also, the pull-in voltage for the dual-beam design is less sensitive to the gap variation.

FABRICATION

Dual-beam relays are fabricated using the process described in [2] at the Stanford Nanofabrication Facility. The platinum conductive layer used in [2] is replaced with a 40 nm-thick titanium nitride (TiN) layer, deposited using atomic layer deposition. A silicon nitride hard mask is used to protect the TiN layer during the isolation etch. The silicon nitride mask layer is etched by a timed exposure to a BOE solution (38% NH4F, 2.5% HF, and 60% water.) for 3 minutes. The TiN is then etched using a timed wet-etch in a 1:2:97 NH_4OH: H_2O_2: H_2O solution for 60 seconds. A close-up image of the isolation etch is shown in Figure 2b. Because the the TiN etch does not depend on a physical etch stop, the isolation etch can spread away from the exposed area of the hard mask. However, because the gate does not make electrical contact with any other surface, damage to the TiN layer on the gate does not affect the performance of the device. After the isolation etch, the device is released in 49% HF then dried in a critical point dryer.

EXPERIMENTAL RESULTS

All devices were stored in a dry nitrogen ambient immediately after release to limit exposure to humidity and oxidizing agents. The relays were tested in an enclosed nitrogen glovebox using a Keithley Parameter Analyzer (4200SCS). During testing, the devices were also monitored visually using a high power microscope. The bias voltage across the source-drain contact was limited to 4 V, and a 100nA compliance was imposed in order to protect the devices from accidental damage.

The I_{DS}-V_B curve for a body voltage sweep is shown in Figure 7. The body voltage was increased to 27V with a step size of 0.25V, while the gate voltage was set to zero. The device pulled in at 24.5 volts and pulled out at 10.5 volts. The current across the gate electrode is also shown, and it remains at noise level throughout the sweep. Given the 4 volt bias across the contact between the drain and the gate during pull-in, the corresponding resistance of the isolation etch on the gate would be in the terra-ohm range.

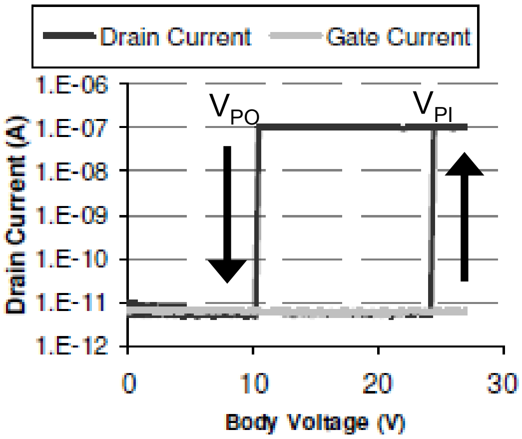

Figure 7: The Current-Voltage response for a sweep of the body voltage with an isolated typical dual-beam device

The relay can also be actuated by imposing a bias on the body terminal while sweeping the gate, as shown in Figure 8a. In this configuration, an inverter can be implemented. When the gate voltage is near VB_{LOW}, the gate pulls in to the VB_{HIGH} electrode and connects V_{OUT} to VDD. When the gate voltage is near VB_{HIGH}, the gate pulls in to the opposing side and VOUT is set to zero volts. The experimental results of inverter testing at different gate biases are shown in Figure 8b.

During testing, devices would sometimes fail to pull-out. For the single-beam devices, such a failure would be irreversible. However, the dual-beam device has a built-in resurrection mechanism. The gate beam, which is still free to move, can be used to hammer the drain and break the contact between the drain and source.

CONCLUSION

A robust six-terminal relay has been successfully designed and tested. This design protects the contact region from damage due to the isolation etch, reduces the effect of gap size variation and reduces the number of contacts in the signal pathway. It also provides a new method of recovery from stiction and welding failure. The design has been used to demonstrate an inverter.

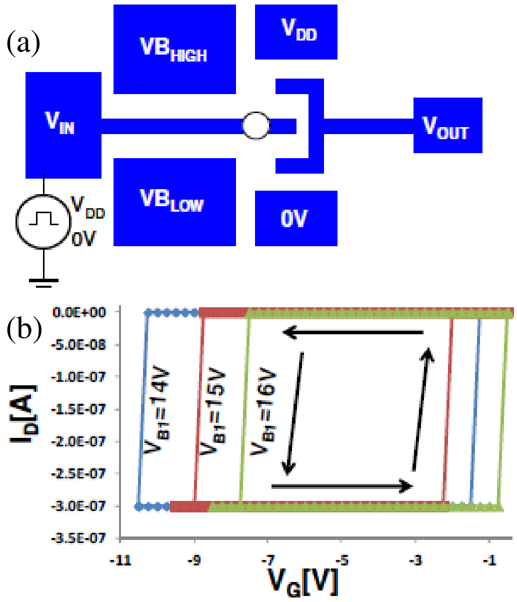

Figure 8: (a) Schematic of a gate-sweep inverter; (b) Inverter response with varying bias at the gate electrodes

ACKNOWLEDGEMENTS

Fabrication was performed at the Stanford Nanofabrication Facility, a member of the National nanotechnology Infrastructure Network, which is supported by the NSF. Images were taken using equipment at the Stanford Nano-Characterization facility. Funding for this research was provided by DARPA MTO program "Nano Electro Mechanical Computers (NEMS)" (Contact Number: NBCH 1090002, Program Manager: Dr. T. Akinwande). K.L. Harrison would also like to thank the NSF GRFP and Ford Foundation for their generous support.

REFERENCES

[1] K. Akarvardar et al. "Design Considerations for Complementary Nanoelectromechanical Logic Gates," *IEEE International Electron Devices Meeting, IEDM 2007*, pp. 299-302, 10-12 Dec. 2007.

[2] Lee et al., "Dual Sidewall Lateral Nanoelectromechanical Relays with Beam Isolation," in *Digest Tech. Papers Transducers '11 Conference,* Beijing, China, June 5-9 2011, pp. 2606-2609.

[3] Pott, V. et al., "Mechanical Computing Redux: Relays for Integrated Circuit Applications", *Proc. the IEEE, Vol. 98, no. 12,* pp.2076-2094, Dec. 2010.

[4] C. Chen et al. "Nano-Electromechanical Relays for FPGA Routing: Experimental Demonstration and Design Technique," DATE (2012).

K.L. Harrison
tel: +1-617-285-7552
email: KLHarris@stanford.edu